REDUCING NEUTRON EMISSION FROM SMALL FUSION ROCKET ENGINES

S.A. Cohen

Princeton Plasma Physics Laboratory, USA, scohen@PPPL.gov

M. Chu-Cheong[*], R. Feder[t], K. Griffin[*], M. Khodak[*], J. Klabacha[t], E. Meier[:t], S. Newbury[◁Jl], M. Paluszek[§], T. Rognlien[:t], S. Thomas[§], and M. Walsh[*]

The mainstream efforts to generate electrical power *via* fusion, represented by the ITER and NIF projects, would use a deuterium-tritium (D-T) fuel mixture to produce energy; the neutrons therein generated would breed the needed tritium. Such approaches to fusion power are predicted to result in large, massive (> 500 mT), and high power (GW) reactors, ill suited for spacecraft missions envisaged for this century. We have been investigating a different fusion reactor concept based on an advanced-fuel (D-^{3}He), RF-heated, field-reversed configuration (FRC) and find that small, relatively low power (1-10 MW) reactors with high specific power are possible and are suitable for a variety of missions throughout the solar system and beyond. Herein we describe the methods to reduce neutron emission to below 1% of the fusion power, thereby reducing the thickness of shielding required to 20 cm and increasing the longevity of the components and the specific power.

I. INTRODUCTION

Spacecraft missions considered for this century include explorations within our solar system, throughout the Oort cloud (10^3-10^5 AU), and even to the nearest stars, *e.g.,* Alpha Centauri[1] (4.4 ly). Whether the missions are within the solar system or beyond, whether they are manned or unmanned, and whether they are flyby, rendezvous or round trip, all strongly benefit from rapid transit times. The shorter the duration the trip, the less exposure of humans to reduced gravity and high radiation, the lower the costs of earth-based mission-control and surveillance tasks and of the initial launch, and the more rapidly the mission objective can be accomplished. The latter is particularly important for planetary defense, specifically, the deflection of comets[2] or large asteroids away from earth-impact trajectories.

When designing rocket engines necessary for these missions, a tradeoff must be made between specific impulse (I_{sp}), thrust, and power capabilities, constrained by the required trip duration and payload and balance-of-system (BOS) masses. These define the specific power (P_{sp}) required. The Δv for solar system missions is in the range 10^4-10^5 m/s. For a payload mass 5-20% of the BOS, the propellant exhaust velocity should be close to Δv, corresponding to an energy in the range of 10-300 eV/amu. Propellant speeds greatly exceeding Δv, cause a major penalty in the power requirement.

A survey of rocket-engine performance for solar-system missions beyond the moon-earth system has compared chemical and nuclear (fission and fusion) power sources.[3] One conclusion reached is that chemical rockets have reached their practical limits, epitomized by long-duration, low-payload-mass missions, such as the New Horizons and Curiosity (Mars) Rover. A corollary is that nuclear power will be needed for more ambitious missions. They state that nuclear electric propulsion is limited by thermal inefficiencies and that fusion could provide more and better mission options because of its higher (theoretical) power conversion efficiency and higher energy-content fuel.

In this paper we concentrate on one technical aspect of fusion-powered rockets: how much mass must be dedicated to shielding from the neutrons released by fusion reactions. Shielding *may* be necessary for human safety, if the missions are manned, but is definitely *essential* to reduce damage to components of the rocket engine that are near the fusing plasma. Fusion power plants for terrestrial use most often are designed to burn the D-T fuel mixture because of its lower required temperature for fusion, *ca.* 10 keV, and the possibility of breeding T in a ^{6}Li-containing blanket that

---

[*] Princeton University, USA
[t] Princeton Plasma Physics Laboratory, USA
[:t] Lawrence Livermore National Laboratory, USA
[§] Princeton Satellite Systems, USA
[◁Jl] Harvard College, USA

surrounds the plasma. For spacecraft having ~10-mT-payload missions of 3-years duration and $\Delta v \sim 10^5$ m/s, the required T is nearly 1 kg. The required power and thrust are relatively low, to 5 MW and 50 N respectively. Tritium breeding is not necessary – the half-life of T is 12.3 years and the "readily" available T supply, currently 22 kg,[4] is sufficient for 0.7 GW of fusion power production for one year. This is a reprieve – T breeding would considerably increase a rocket's complexity and mass.

However, energetic (14.1 MeV) neutrons are produced by D-T fusion, Eqn. [1].

$$D + T \quad \rightarrow {}^4He\ (3.5\ MeV) \quad + n(14.1\ MeV) \quad [1]$$

The damage fast neutrons create in materials is substantial. For structural materials, like stainless steel, the tolerable damage is ~60 displacements per atom (DPA),[5] about the peak dose that the inner wall of a tokamak reactor would receive in one month of full power operation at a neutron wall load of 4 MW/m². Other materials are far more sensitive to DPA. Notably, high-temperature superconductors (Hi-T SC) can tolerate far less damage, ~ 0.5 DPA, before their properties begin to degrade. Thus while stainless steel structures requires "only" 0.8 m of (typically ^{10}B) shielding, superconductors would require about 1.1 m to be functional for one full-power year.

In Section II of this paper we describe several sequential changes in the design of a fusion reactor, from a large D-T burning (ITER-like)[6] tokamak (which has problems well beyond neutron damage with respect to its use as a rocket engine in this century) to a small D-^{3}He fueled FRC. Overall, these changes would reduce the neutron flux to the first wall by a factor of 1000. In Section III, we evaluate the required shielding, using a neutron transport code that considers material-dependent DPA, nuclear heating, and nuclear transmutations (including H and He generation and bubble/void formation). We find that the required shielding thickness is near 0.2 m, for one full-power year. This allows a 5-fold reduction in shielding weight compared to D-T operation (of the same reactor) and plays an important role in determining for which missions this type of rocket would be useful.

II. REDUCING NEUTRON FLUXES

The most common method suggested to reduce neutron emission is to change the fuel mixture to D-^{3}He or p-^{11}B. We discount p-^{11}B. It is unlikely to produce net energy because of the high plasma temperature required, the low energy release *per* fusion event, and the reduction in reactive nuclei density (at fixed electron density) due to the high Z of the B. D-^{3}He fusion, Eqn. [2], does not have

those shortcomings[7] but does promote neutron production through two routes: one channel of D-D fusion, Eqn. [3]; and fusion of the T "ash" created by the other D-D fusion channel, Eqn. [4]. A method will be described later in this section to remove the unavoidable T ash before it fuses.

$$D + {}^3He \quad \rightarrow {}^4He(3.6\ MeV) \quad + p(14.7\ MeV) \quad [2]$$
$$D + \ D \quad \rightarrow {}^3He(0.82\ MeV) + n(2.45\ MeV) \quad [3]$$
$$D + \ D \quad \rightarrow \ T(1.01\ MeV) \quad + p(3.02\ MeV) \quad [4]$$

We now describe steps to reduce neutron production and wall load. Some of these steps do not immediately reduce the neutron wall load but are necessary for the subsequent steps to work.

The small FRC

The tokamak approach to fusion propulsion requires a large device, producing GWs of power,[8] a level far in excess of spacecraft propulsion needs in *this* century. Simply lifting tokamak components to LEO would be exorbitantly expensive, *ca.* 100B$. Moreover, the tokamak, unlike the mirror machine,[9] does not possess a geometry naturally suited for the direct conversion of fusion power to thrust. We instead choose the FRC[10] (Fig. 1) in which a closed-field-line region (CFR), not unlike a tokamak's, is embedded in the open-field-line region (OFR) of a mirror machine. This union gains confinement benefits from the CFR and power-to-thrust conversion capability from the OFR.

A large D-T burning FRC does not reduce the neutron wall load. In fact, it increases it, by having less wall area. However, FRC reactors could be smaller because their energy confinement is expected, and recently shown by experiments,[11] to be to be classical, about $(1+q)^2 \sim 10$ times better than a tokamak's (neoclassical) because the q (safety factor $\propto$ toroidal field) of an FRC is 0 while that of a tokamak is near 3.

A smaller fusion reactor ameliorates several problems immediately. Firstly, it reduces the power approximately proportional to the plasma volume, hence the plasma edge radius (r_s) cubed, bringing it into the range of powers, 1-10 MW or modules thereof, considered appropriate for many of this century's solar system missions. The size reduction reduces cost commensurably.

Secondly it reduces the neutron wall load by the surface-to-volume ratio, $\propto 1/r_s$. For constant fusion power density, a small FRC, one whose size was consistent with near-classical energy confinement, would have about a five-fold reduction in neutron wall load.

A third benefit gained by choosing a small reactor is improved stability. Early FRC plasmas,
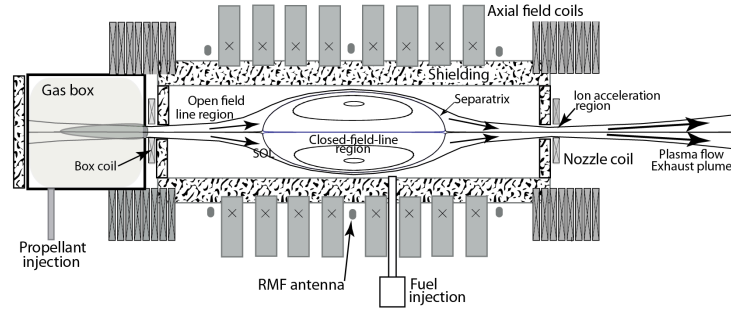
Fig. 1. Schematic of an FRC rocket engine. Fusion occurs in the closed-field-line region. Propellant is added in the gas box where it is ionized; that plasma then flow along field lines in the open-field-line region (SOL) and across the separatrix surface of the CFR where its electrons are heated. The propellant ions are accelerated axially as they pass through the nozzle coil. Fuel is injected into the FRC core by ~20 keV neutral beams. The magnet coils are in a linear array, with gaps between segments.

ones formed by the theta-pinch method, often terminated in less than 100 μs, a time attributed to the internal tilt mode. This is an MHD instability predicted[12,13] to be pernicious when the ion gyroradius (ρ_i) is a small fraction, typically less than 1/10 of the FRC's minor radius ($s \approx 0.3 \, r_s/\rho_i > 10$). With a small FRC, the value of s for the thermal plasma can be kept near or below 10 for the fuel and 3 for the fusion products. Recent low-s FRC experiments have sustained plasmas for 3 to 300 ms,[14,15] over 10^5 times longer than the growth time of the internal tilt mode for larger radii FRC having the same plasma parameters and magnetic field.

A fourth benefit of small FRCs, one related to T exhaust, will be discussed in the next subsection.

Before that, we note that a special plasma heating method is essential to allow small steady-state FRCs. The commonly used neutral-beam-injection technique, at energies in excess of 100 keV, requires large plasmas, $r_s > 1$ m, to absorb the power. We instead choose an RF method called odd-parity rotating magnetic fields (RMF_o).[16,17] RMF_o has been shown, experimentally, to heat electrons efficiently.[18] Ion heating is predicted and experimental tests are under way. RMF_o is also predicted to allow improved energy confinement by maintaining closed field lines in the CFR. Typical parameters for the rocket engine are in Table I and have been discussed in previous papers.[19,20,21,22] The required energy confinement time is less than classical by a factor of 2.5. Two modes of operation will be discussed in this paper, one with the all ions in thermal equilibrium at 70 keV, the other with non-thermal distributions and the peak ^{3}He energy twice that of the D, a result predicted for RMF_o-heated D-^{3}He plasmas.[23] This reactor is driven, *i.e.,* the RMF_o continually supplies power to heat the plasma and to sustain the current – accruing the benefit that no loss of plasma control

Table 1. Typical FRC rocket engine parameters

Separatrix radius, r_s	0.25 m
Elongation, κ	5
Central magnetic field	6.6 T
Plasma current	10 MA
Electron density	5×10^{20} m^{-3}
^{3}He:D ratio	3
Deuterium temperature	70 keV
^{3}He temperature	70-140 keV
Electron temperature	30 keV
SOL density	$5\text{-}50 \times 10^{19}$ m^{-3}
SOL temperature	20-120 eV
s_{fuel}	10
s_T	3.3
$<\beta>$	0.84
RMF_o power	1 MW
Fusion power	5.2 MW
^{3}He burn-up rate	0.26 kg/yr
Radiation losses	3.1 MW
Radiation load on wall	0.62 MW/m^2
$\tau_E/\tau_{E,classical}$	0.4
Gas box power load	1.0 MW
Energy recovery efficiency	40%
Thrust power	2.1 MW
Excess power available	0.4 MW
Isp	3×10^4 s
Propellant (D) consumed	to 10^4 kg/yr
% power in neutrons	0.5-0.1%
Neutron wall load	3-0.6 kW/m^2

will occur when fusion events increase or decrease. Power lost from the plasma by synchrotron and Bremsstrahlung radiation to the walls and into the gas box by plasma conduction and convection is converted, at 40% efficiency, to electrical power to be used for the RMF_o. Excess electrical power is available for station keeping, auxiliary thrusters and communications. No credit is taken for wall reflection of synchrotron radiation. By varying the

rate of propellant introduced into the gas box, the SOL density and temperature are controlled, critical to T exhaust. Two cases are shown in figure 2 for an FRC generating 20 MW of power of which 10 MW is deposited in the SOL. Typically, the directed ion energy in the exhaust plume beyond the nozzle is 4x the electron temperature, corresponding to ~500 eV for the case where 10 kA (equiv current) of D neutrals is fed into the gas box.
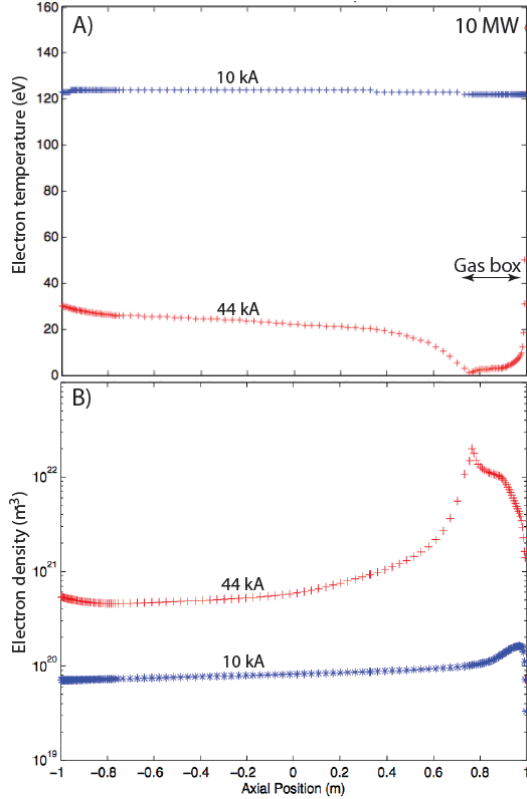

Fig. 2. Results of 1-D UEDGE simulations of FRC SOL parameters. A) T_e *versus* axial position (z) for a 2-m-long FRC that deposits 10 MW into the SOL electrons. Results are shown for two (D_2) propellant-flow rates into the gas box, 10 kA and 44 kA (equivalent current). The gas box is located at an axial position of 0.8-1 m and the nozzle at -1 m. B) Electron density *versus* z. These high densities are required for rapid T^+ removal.

Particularly noteworthy in Table I is the neutron wall load, which is less than 0.1% that commonly specified for tokamak D-T reactors. The next subsections describe how this reduction is created.

D-^{3}He fuel and T ash removal
^{3}He, though rare, is less scarce on earth than T because ^{3}He does not undergo radioactive decay.

About 70 kg are currently available and an additional 5 kg are produced annually, mostly by decay of T produced at heavy water reactors.[24] Thus ample D-^{3}He is available for several 1-10-MW, 1-year-duration missions.

A 1:1 D:^{3}He fuel mixture directly produces copious neutrons *via* Eqn [3]. These neutrons, though 1/6 as energetic as D-T's 14.1 MeV neutrons, still cause damage in materials. Wittenberg, *et al.*[25] have calculated the reduction in neutron production gained by changing the mix ratio. A lower D fraction dramatically cuts the 2.45 MeV neutron production rate, though a penalty is paid in fusion power. By choosing a ratio of 1:3 and an ion temperature of 70 keV, the percentage of fusion power in the 2.45 MeV neutrons is 1%. However, the T produced *via* Eqn. [4] must be removed quickly compared to its characteristic burn-up time, *ca.* 20 s. We now explain how this will happen naturally in small FRC reactors.

Figure 3A shows the trajectory of a slowing-down T^+ fusion product in a 25-cm-radius FRC. Because of their low *s* value, *ca.* 3, the vast majority of energetic fusion-product T^+ pass across the FRC separatrix and traverse the OFR, also called the scrape-off layer (SOL). The SOL plasma is considerably colder than in the core because the open field lines allow unimpeded plasma energy losses. Simulations of the FRC SOL using the UEDGE code show, figure 2, the edge plasma temperature and density to be in the ranges, 20 eV < T_e < 120 eV and 5 x 10^{13} cm^{-3} < n_e < 5 x 10^{14} cm^{-3}, respectively, depending on the propellant input into the gas box. At these values for the SOL plasma parameters, the fusion products slow down in less than 0.01 s. In doing so, their trajectories end up fully in the SOL, see Figure 3B, from where they are promptly expelled with the propellant. (A note of caution, the classical slowing-down rates[26] may have to be modified to take into account the novel regime of this system wherein the Debye length is longer than the electron gyro-radius. Kinetic calculations on this are in progress.)

Non-thermal ion distributions
The above changes reduce the neutron first wall load to 3 kW/m^2, less than 0.1% that in a D-T tokamak reactor. (The photon radiation load on the wall, 0.62 MW/m^2, is lower than in a tokamak reactor by a factor of 8.) We have been investigating whether a further reduction in neutron generation may naturally occur because of the nature of RMF$_o$ heating. Hamiltonian simulations show that ions are periodically energized then cooled[17,23] as the RMF$_o$ rotates around the FRC at a frequency near 1 MHz.
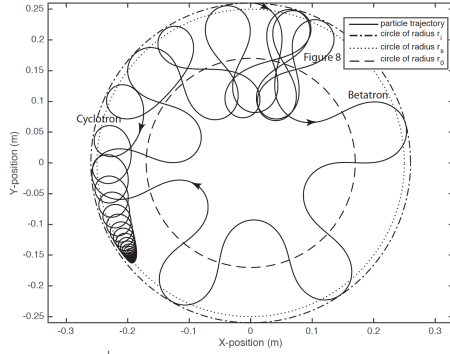
Fig. 3A. T$^+$ fusion-product trajectory mapped onto the FRC's z = 0 midplane. Slowing down, *via* electron drag, occurs in the SOL, located between the circles at r_s = 25 and r_i = 26 cm. The T$^+$'s trajectory changes from betatron to figure 8 to cyclotron orbit. (The slowing-down rate has been artificially accelerated to show the transitions between these orbit types.)
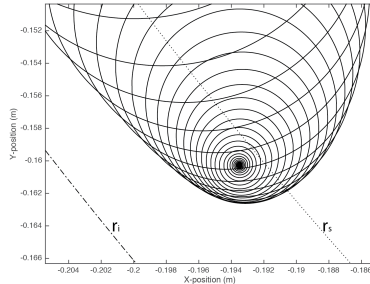

Fig. 3B. Close-up view of the cyclotron segment of the T$^+$orbit, showing that the orbit eventually lies fully in the SOL.

Ions with higher Z are accelerated to higher energy. Each ion species forms a beam in the rotating potential well created by the RMF$_o$ and periodically drift away from then back into the well at the RMF$_o$ frequency. Different ion species have different beam velocities. D-D collisions are within the D beam, hence are at a lower center-of-mass energy than in a Maxwellian plasma. In contrast, D-^{3}He collisions are between two beams, hence are at a higher center-of-mass energy. We estimate that this effect could reduce the T- and n-producing D-D fusion events by a factor of 6. This benefit would not come without a penalty. Rider[27] has noted that, based on thermodynamic principles, power is required to maintain ion distributions at different average energies. Whether the RMF$_o$ can do this efficiently awaits self-consistent calculations and experimental tests.

III. CALCULATING SHIELDING REQUIREMENTS

In this section we report quantitative computations of how much and what type of shielding is needed to protect the reactor's superconducting magnet coils from neutron damage and heat load. We assume that the neutron generation rate is 1% of the fusion power, a factor of 2 larger than the primary case described in Section II. To balance this excess, for these calculations we set the generated fusion power at 1 MW/m, a factor of 2 lower than the parameters in Table 1.

By means of neutron transport analysis with the ATTILA code, we show that, based on displacements-per-atom (DPA), 20 cm of $^{10}B_4C$ shielding would protect the central magnet coils in a 1 MW/m FRC for one year of continuous operation to a dose of 6 x 10^{17} n/cm^2. Natural boron has an isotopic composition of 80% ^{11}B and 20% ^{10}B. In the energy range 1-10 MeV, the ^{10}B n-absorption cross is more than 10^4 times larger than ^{11}B's, hence increasing ^{10}B content will reduce the amount of shielding necessary. (In this paper, "enriched" $\equiv$ 100% ^{10}B.)

Types of neutron damage in materials are shown in figure 4. Other neutron effects, *e.g.,* He^4-build-up and heat load, were also quantified and found to be less important than DPA.
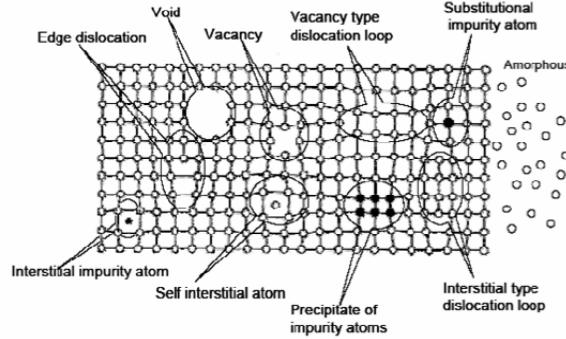

Fig. 4. Types of neutron-induced damage.

The neutron fluences and their effects were computed for a variety of shielding configurations and shielding materials, *e.g.,* W inserts (used to absorb the X-rays) and isotopically enriched B$_4$C. The effects of neutron fluence on other reactor components, *e.g.,* the vacuum vessel (VV) wall, the B$_4$C shielding, and the RF antenna used for plasma heating and current drive, were also investigated. In all cases, DPA was the most important lifetime-affecting factor. Heating due to the neutron load was minor. Bremsstrahlung and synchrotron radiation from the plasma provides a far larger heat load on the vessel walls and thus dominates design choices for wall cooling. Importantly, the OSHA-specified limits for human exposure necessitates 50-cm thicker shielding that the Hi-T SC coil DPA requirement, if humans were to be present within 1.1 m of the reactor for periods greater than 1 month *per* year.

5

The model

The particle simulation software ATTILA[28,29] was used to analyze the effects of neutron radiation on the materials of the reactor as well as potential hazards to humans in the vicinity of the reactor. ATTILA uses Chebyshev-Legendre quadrature to solve a particle transport problem in space, angle, and energy. The model geometry, including material prescriptions, is given to the program and divided into a finite element mesh. The precision of the solution can be adjusted by refining the mesh as well as controlling the order of the polynomials used in both angular quadrature and the scattering of particles and the fineness of the energy groups of particles that are used. ATTILA has a library of energy-dependent neutron cross-sections for over 100 different materials, prepared for the ITER project. The displacements-per-atom reaction rate, activation products, helium production, and heat deposition rates are unique to each material.

Geometric symmetries were used so that only a portion of the reactor had to be modeled. One model is a 90-degree cylindrical sector (see figure 5). This model assumed that the reactor was an infinitely long cylinder; accordingly it used reflecting boundary conditions on the four end faces. The neutron radiation was assumed to be uniform throughout a cylindrical region within the 25-cm radius plasma and spanning the length of the reactor.
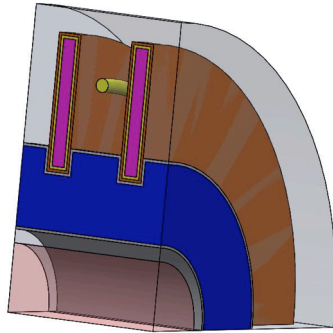

Fig. 5. 90°-segment cylindrical model of the FRC reactor. The plasma radius is 25 cm. The B_4C shielding begins at 32 cm and extends outward. Two axial field coils are shown as well as one RMF_o antenna segment.

The other primary model is a 10-degree sector of the full length of an ellipsoidal FRC, with reflecting boundary conditions on the two side faces of the slice. B_4C caps are added at the ends of the FRCs VV, with axial holes at the nozzle coils for the propellant supply and exhaust (see figure 6).

The fusion region of the reactor is ellipsoidal within this cylindrical space, a shape set by the magnetic fields.
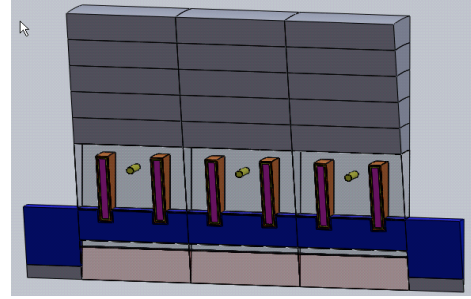

Fig. 6. 10°-segment ellipsoidal FRC reactor model. The plasma ellipsoid has a 25-cm midplane radius. The B_4C shielding is cylindrical along the length. The ends of the cylinder are capped with B_4C-lined nozzles. Losses out the nozzles are evaluated. Six axial field coils are shown as well as three RMF_o antenna segments.

Results

The critical temperature of YBCO superconductors decreases linearly with fluence;[30] the critical current falls in a similar fashion, after a slight improvement at very low fluences. Un-irradiated YBCO has a critical temperature of 105K. It is desired that the critical temperature not fall substantially, because this would require the implementation of a liquid neon or helium cooling system, which would add cost and complexity to the project. Maintaining a critical temperature above 77K is a conservative target for designing shielding, simplifying terrestrial testing of the system. A fluence of 5.4×10^{18} n/cm^2 drops the critical temperature to 77 K. Fixing the maximum allowable fluence at 6×10^{17} $/cm^2$ – which will degrade the T_c and I_c performance 10% towards the minimum allowable value – allows margin for degradation from other sources such as solar radiation. Figure 7 shows the flux distribution.

Conductor Fluence

With the limit set for YBCO at 6×10^{17} neutrons/cm^2, a 1-year full-power exposure requires 20 cm of shielding while a 30-year life span would require 33 cm of enriched shielding or 39 cm of natural B_4C shielding to stay below this fluence (see figure 8). Enriching the shielding from 80% ^{11}B and 20% ^{10}B to 100% ^{10}B is more effective at decreasing conductor fluence than adding a 0.5 cm tungsten layer between the plasma and the shielding. Enriching the shielding decreases conductor fluence by between 50% and 75% (depending on the

shielding thickness). Meanwhile, adding a tungsten layer only decreases conductor fluence by between 7% and 14%. All three shielding grades provide adequate protection, but the [10]B enriched shielding, as expected, yields the lowest neutron fluences and thus will provide the lowest losses in superconductor performance and the most efficient liquid-nitrogen cooling system.
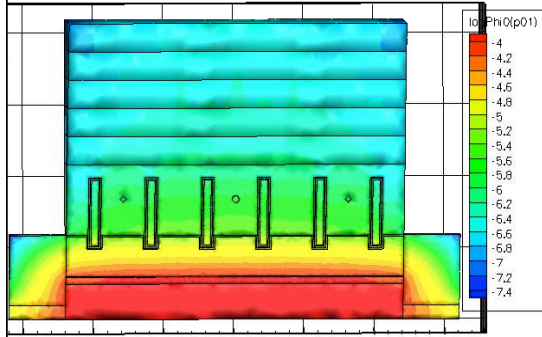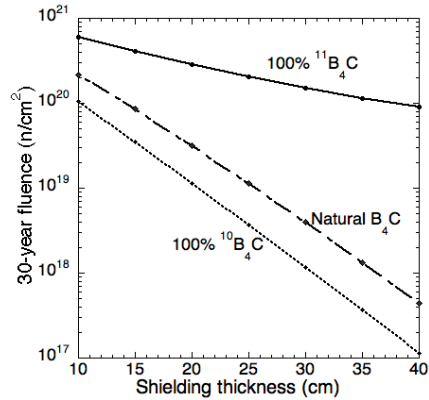

Fig. 7. Flux distribution with 20 cm B_4C.

Fig. 8. Peak neutron fluence as function of shielding material and thickness for a 30-year full-power exposure.

Nuclear Heating

Nuclear heating values due to neutron flux are small relative to the heating due to Bremsstrahlung and synchrotron radiation, which together contribute 30 times greater heating than the neutrons. When multiplied by the volume of the component, heating values for the conductors and RF antenna are less than 121 W, which is very small compared to the 2.4 MW output of the reactor (see figure 9 and Table 2). The total heating in the shielding and tungsten cooling elements is about 40 kW, which is also small compared to the Bremsstrahlung power absorbed. Similarly to the effect for fluence, enriching the shielding is more effective at decreasing conductor heating than adding a tungsten layer. Enriching the shielding decreases conductor

heating by between 46% and 64% (depending on the shielding thickness). Adding a tungsten layer only decreases heating by between 7.5% and 7.8%.
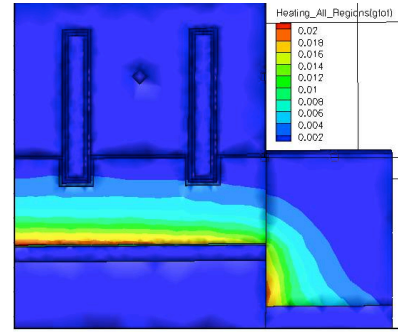

Fig. 9. Contours of neutron-induced heating.

Table 2. Maximum heating (W/cc): 20 cm B_4C

YBCO	Inner VV	B_4C (center)	B_4C (Nozzles)
2.4e-4	9.5e-3	2.2e-2	2.0e-2

Helium Production

All helium production – from (n,α) reactions – values are smaller than 1 ppm produced *per* year (figure 11). Copper is not noticeably embrittled at < 1 He ppm.[31] Steel is even more resilient to He embrittlement.[32] Both the RF antenna and conductor coating that encases the YBCO superconductor ribbon will be insignificantly affected with any of these shielding thicknesses or materials. It is possible that the helium production will be a problem in the B_4C shielding, but could be mitigated with channels or porosity designed to carry helium out of the solid.
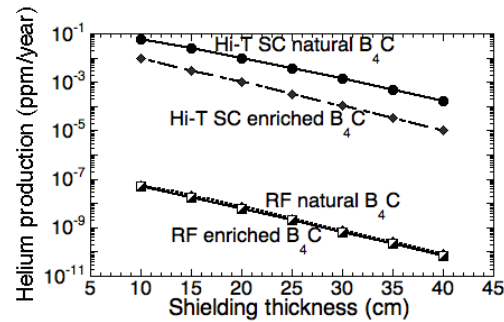

Fig. 11. Neutron-induced helium production.

Neutron Losses

For both shielding materials, the percentage of neutrons that escape through the axial ports is small, *ca.* ½ %, compared to the total number produced, see figure 12. Thirty percent fewer neutrons escape when enriched shielding is used. The energy distribution of escaping neutrons (figure 13) is relatively mild; accordingly, less than 10 cm of shielding will be needed for the gas box.
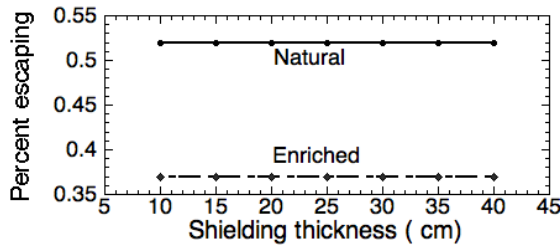
Fig. 12. Percent of neutrons escaping through both end caps holes *versus* the thickness of natural and enriched B_4C shielding.
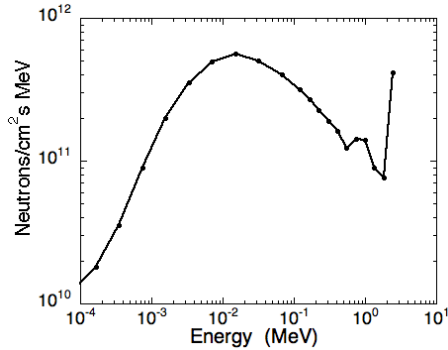

Fig. 13. Energy spectrum of escaping neutrons.

Displacements per Atom

All values are exceptionally low (< 0.1dpa produced per year) and will not contribute to structural deterioration (see figures 14 and 15).[30] The superconductors will experience decreased performance at high DPA values.[33] Although tolerable DPA levels are not yet known with precision, the results from conductor fluence experiments suggest that approximately 33 cm of enriched shielding or 39 cm of natural B_4C shielding are required to remain within 5% of maximum (un-irradiated) performance for 30-year exposures and 20 cm for a 1-year exposure.
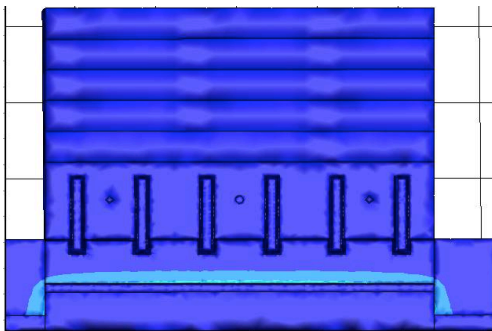

Fig. 14. Contours of DPA. Most damage is confined to the first ~ 4 cm of the shield.

The conductor DPA results are calculated using the material properties of Nb_3Sn because the material properties of YBCO were not available.

Thus conductor DPA values must be interpreted as approximations rather than precise. A detailed experimental study of the effects of DPA on Hi-T SC performance is required to determine the precise DPA limits for the superconductors.
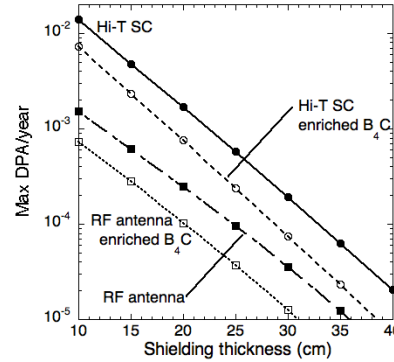

Fig 15. DPA *versus* shield thickness for the Hi-T SC and RF antennae.

Human Exposure

Acceptable values for human exposure depend on the how often and for how long human operators will be in the vicinity of and how close they will be to the reactor. Adding 50 cm of shielding increases safe radiation exposure times by more than 3 orders of magnitude (see figure 16). After that, each additional 20 cm of shielding outside around the coils increases safe exposure times by another two orders of magnitude. With 1.09 m of total shielding, humans could safely spend 44% of their working hours 1.09 m from the reactor.
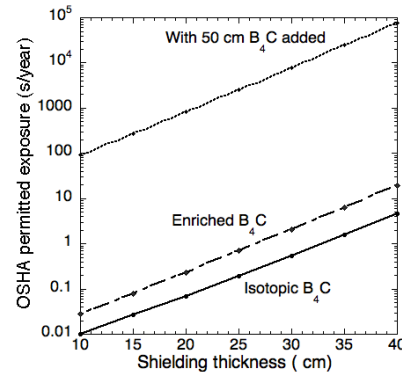

Fig. 16. OSHA-permitted human exposure time at 1.09 m from the FRC reactor, *versus* shielding thickness and type. Only with 50 cm of enriched B_4C *added* (to 30 or 40 cm), could humans work near the rocket engine for appreciable time.

IV. SAMPLE MISSION

NASA is studying a mission to land two identical robotic spacecraft on the surface of Jupiter's moon Europa. Europa might harbor life in its ocean of liquid water beneath its icy shell. The NASA mission, as currently described, would take 6 years to reach Jupiter while an FRC direct-fusion-drive (DFD) propelled mission would reach Europa in 1 year. It would go into orbit around Europa; two landers would descend from the orbiter to the surface. The landers would be powered by laser or RF beamed from the orbiter. The high electric power available on the orbiter would allow for drilling through the icy shell to the ocean. Parameters of the mission are listed in Table 3, assuming the rocket engine described in Table 1.

Table 3. Europa obiter/landers mission

Masses	
Vacuum vessel	800 kg
Magnets	300 kg
RF power generation system	1050 kg
Heat rejection system	425 kg
Thermal power conversion system	2200 kg
Shielding	3200 kg
Total engine mass	**7975 kg**
Propellant	2000 kg
Payload	1000 kg
Isp	30,000 s
Mission duration	1 year
Thrust	20 N
Fusion power	5 MW

Without T removal accomplished by control of the SOL, the mass of the shielding would increase 5 fold and the specific power fall a factor of 3. The mission would become impractical.

.
V. SUMMARY

The idea to use fusion to power spacecraft is almost 50 years old.[34] Most concepts describe GW power levels,[3,8,35] based on the leading research elements in DOE's fusion program and whose extensive experimental results allow more confidence in the parameters that could be achieved in a fusion power plant. The mainline fusion program currently concentrates on the tokamak device and laser fusion (NIF).[36] Building a space-propulsion system today, based on either, could be viewed as building Cunard Line's *Queen Mary* back in the late 15th century, in support of Christopher Columbus's plans, when a far smaller vessel, the *Santa Maria,* was all that was needed and all that was technically and financially feasible.

In recent years, advances in fusion research on high-β compact toroids have motivated us to investigate still ambitious and challenging missions possible with smaller fusion-powered rocket engines. We have previously provided analyses of unique missions for which a relatively small, 1-10 MW, fusion-powered rocket could provide the required thrust, Isp, and specific power: exploring Jupiter's icy moons, a manned orbiter mission to Mars, positioning the James Webb space telescope at the L-2 point, asteroid intervention, and, most recently, an exploration of Pluto and beyond.

A critically important question in evaluating these missions is neutron shielding. The mass of the required shielding depends not only on the fuel mixture but also on the details of reactor design and operation. Specifically, though D-^{3}He fusion, Eqn. [2], produces no direct neutrons, the co-existent D-D reactions do, *via* Eqn. [3] and, more importantly, the fusion of T ash, Eqn. [4]. Without removing the T produced and minimizing the D-D fusions in general, hardly a gain is derived from D-^{3}He fuel.

For a reactor to benefit from D-^{3}He fueling, it must naturally exhaust T ash before fuses. Compared to T-suppressed fusion,[37,38] D-T or D-^{3}He fusion (without T suppression) would increase the shielding mass necessary to safeguard rocket engine components near the fusing plasma by a factor of 5.

Herein, we have described a sequence of changes in reactor design elements, based on small, low-*s,* RF-heated FRCs with specific SOL parameters, for rapid removal of T ash formed by D-D fusion. Critically, the ability to increase the SOL plasma density and reduce its temperature by the injection of propellant into the gas box allows the rapid removal of T from the plasma. Serendipitously, the SOL parameters proper for T removal provide the desired Isp and thrust for a compelling range of missions. The result of tritium removal is a thousand-fold reduction in neutron power load on the first wall, compared to a D-T tokamak.

The most sensitive component found by these analyses is the Hi-TSC used in the axial-field magnets. By implementing the above design changes, the mass of shielding for superconducting coils can be significantly reduced. Further reductions may be possible, such as by using pure B instead of B_4C, by moving the Hi-T SC coils further from the plasma, and by tailoring the shielding thickness to match the local neutron generation rate.

References

[1] http://100yss.org/symposium/2015

[2] Wurden, G., *et al.,* "A new vision for fusion energy research: fusion rocket engines for planetary defense," to appear in J. Fus. Energy.

[3] Cassibry, J., *et al.,* " Case and development path for fusion propulsion," J. Spacecraft and Rockets **52**, 595 (2015).

[4] Van Dam, J.W., "The scientific challenges of burning plasma," Invited talk, DPP-APS, Orlando (2007).

[5] Was, G. S., *Fundamentals of Radiation Material Science*, Springer-Verlag, Berlin Heidelberg (2007).

[6] Campbell, D.J., "Preface to Special Topic: ITER," Phys. Plasmas **22**, 021701 (2015).

[7] Santarius, J.F. "Lunar ^{3}He, fusion propulsion and space development," Lunar and Planetary Institute (1992).

[8] Williams, C.H., *et al.,* "Realizing `2001: A Space Odyssey': Piloted spherical torus nuclear fusion propulsion," NASA/TM-2005-213559, AIAA-2001-3805.

[9] Bagryansky, P.A., *et al.,* "Three-fold increase of the bulk electron temperature of plasma discharges in a magnetic mirror device," Phys. Rev. Lett. **114**, 205001 (2015).

[10] M. Tuszewski, "The field reversed configuration," Nucl. Fusion **28**, 2033 (1988).

[11] Binderbauer, M.W., *et al.,* "Dynamic formation of a hot field reversed configuration with improved confinement by supersonic merging of two colliding high-compact toroids," Phys. Rev. Lett. **105**, 045003 (2010).

[12] Rosenbluth, M.N. and Bussac, M.N. "MHD stability of spheromak," Nucl. Fusion **19**, 489 (1978).

[13] Ishida, A., *et al.,* "Variational formulation for a multifluid flowing plasma with application to the internal tilt mode of a field-reversed configuration," Phys. Fluids **31**, 3024 (1988).

[14] Binderbauer, M.W., *et al.,* "A high performance field-reversed configuration," Phys. Plasmas **22**, 056110 (2015).

[15] Cohen, S.A., *et al.,* "Long-pulse operation of the PFRC-2 device," Bull. Am. Phys. Soc. **58**, 128 (2013).

[16] Cohen, S.A and Milroy, R.D., " Maintaining the closed magnetic-field-line topology of a field-reversed configuration with the addition of static transverse magnetic fields," Phys. Plasmas **7**, 2539 (2000).

[17] Glasser, A.H. and Cohen, S.A. "Ion and electron acceleration in the field reversed configuration with an odd-parity rotating magnetic field," Phys. Plasmas **9**, 2093 (2002).

[18] Cohen, S.A., *et al*., "Formation of collisionless high-β plasmas by odd-parity rotating magnetic fields," Phys. Rev. Lett. **98,** 145002 (2007).

[19] Mueller, J.B., *et al.*, "Modular aneutronic fusion engine," Space Propulsion 2012, Bordeaux, France, (2012).

[20] Paluszek, M.A., *et al.*, "Direct fusion drive for a human mars orbital mission," Proc. IAC, Toronto, (2014).

[21] Razin, Y.S., *et al.*, "A direct fusion drive for rocket propulsion," Acta Astronautica **105,** 145 (2014).

[22] Mueller, J.B., *et al.,* "Direct fusion drive rocket for asteroid deflection," Proceedings, IEPC-2013, Washington, (2013).

[23] Cohen, S.A., *et al.,* "Stochastic ion heating in a field-reversed configuration geometry by rotating magnetic fields," Phys. Plasmas **14**, 072508 (2007).

[24] http://w3.pppl.gov/ppst/docs/newbury.pdf

[25] Wittenberg, L.J., *et al.,* "Lunar source of ^{3}He for commercial fusion power," Fus. Techn. **10**, 167 (1986).

[26] Stix, T.H., "Heating of toroidal plasmas by neutral injection," Plasma Phys. **14**, 367 (1972).

[27] Rider, T.H., "Fundamental limitations on plasma fusion systems not in thermodynamic equilibrium," Phys. Plasmas **4**,1039 (1997).

[28] ATTILA: comprehensive radiation transport solution environment, http://www.radiative.com/Attila-010505.pdf.

[29] Youssef, M.Z., *et al,* "Neutronics analysis of the international thermonuclear experimental reactor (ITER) MCNP `Benchmark CAD Model' with the ATTILA discrete ordinance code," Fusion Engineering and Design **83**, 1661 (2008).

[30] Emhofer, J., M. Eisterer, and H. W. Weber. "Stress Dependence of the Critical Currents in Neutron Irradiated (RE)BCO Coated Conductors." Superconductor Science and Technology **26**, 035009 (2013).

[31] Fabritsiev, S. A., *et al*., "Effect of neutron irradiation on the mechanical properties and fracture mode of Cu/SS joints" Plasma Devices and Operations **8**, 225 (2001).

[32] Grimes, R.W., *et al.,* "Greater Tolerance for Nuclear Materials." Nature Materials **7**, 683 (2008).

[33] Weber, H.W., "Radiation Effects of Superconducting Fusion Magnet Components," International Journal of Modern Physics E **20**, 1325 (2011).

[34] Moeckel, W.E., "Comparison of Advanced Propulsion Concepts for Deep Space Exploration," Journal of Spacecraft and Rockets **9**, 863 (1972).

[35] Teller, E., *et al.,* "Space propulsion by fusion in a magnetic dipole," Fusion Technology **22**, 82 (1992).

[36] Lindl, J., "Development of the indirect-drive approach to inertial confinement fusion and the target physics basis for ignition and gain," Phys. Plasmas **2**, 3933 (1995).

[37] Sheffield, J. and Sawan, M., "Deuterium-fueled power plants with tritium suppression," Fusion Sci. Technol. **53**, 780 (2008) .

[38] Kesner, J., *et al.,* "Helium catalyzed D-D fusion in a levitated dipole," Nucl. Fusion **44**, 193 (2004).